Cancer Science
Japanese Cancer Association JCA
Open Access

Differential reactivation of fetal/neonatal genes in mouse liver tumors induced in cirrhotic and non-cirrhotic conditions

Xi Chen,[1] Masahiro Yamamoto,[1] Kiyonaga Fujii,[1] Yasuharu Nagahama,[1] Takako Ooshio,[1] Bing Xin,[1] Yoko Okada,[1] Hiroyuki Furukawa[2] and Yuji Nishikawa[1]

[1]Division of Tumor Pathology, Department of Pathology, Asahikawa Medical University, Asahikawa; [2]Division of Gastroenterological and General Surgery, Department of Surgery, Asahikawa Medical University, Asahikawa, Japan

Key words

Hepatocellular carcinoma, insulin-like growth factor 2, liver cirrhosis, mRNA expression, trefoil factor 3

Correspondence

Yuji Nishikawa, Division of Tumor Pathology, Department of Pathology, Asahikawa Medical University, Higashi 2-1-1-1, Midorigaoka, Asahikawa, Hokkaido 078-8510, Japan.
Tel: +81-166-68-2370; Fax: +81-166-68-2379;
E-mail: nishikwa@asahikawa-med.ac.jp

Funding Information

Ministry of Education, Culture, Sports, Science, and Technology of Japan.

Received January 16, 2015; Revised May 6, 2015; Accepted May 17, 2015

Cancer Sci **106** (2015) 972–981

doi: 10.1111/cas.12700

Hepatocellular carcinoma develops in either chronically injured or seemingly intact livers. To explore the tumorigenic mechanisms underlying these different conditions, we compared the mRNA expression profiles of mouse hepatocellular tumors induced by the repeated injection of CCl_4 or a single diethylnitrosamine (DEN) injection using a cDNA microarray. We identified tumor-associated genes that were expressed differentially in the cirrhotic CCl_4 model (*H19*, *Igf2*, *Cbr3*, and *Krt20*) and the non-cirrhotic DEN model (*Tff3*, *Akr1c18*, *Gpc3*, *Afp*, and *Abcd2*) as well as genes that were expressed comparably in both models (*Ly6d*, *Slpi*, *Spink3*, *Scd2*, and *Cpe*). The levels and patterns of mRNA expression of these genes were validated by quantitative RT-PCR analyses. Most of these genes were highly expressed in mouse livers during the fetal/neonatal periods. We also examined the mRNA expression of these genes in mouse tumors induced by thioacetamide, another cirrhotic inducer, and those that developed spontaneously in non-cirrhotic livers and found that they shared a similar expression profile as that observed in CCl_4-induced and DEN-induced tumors, respectively. There was a close relationship between the expression levels of *Igf2* and *H19* mRNA, which were activated in the cirrhotic models. Our results show that mouse liver tumors reactivate fetal/neonatal genes, some of which are specific to cirrhotic or non-cirrhotic modes of pathogenesis.

Various risk factors for hepatocellular carcinoma (HCC) exist, including infection with hepatitis B virus (HBV) and hepatitis C virus, alcoholic and non-alcoholic fatty liver disease, and several hereditary metabolic diseases.[1] However, chronic liver injury, typically cirrhosis, is the most important and common setting for the development of HCC. Although recent studies have revealed critical roles of the interleukin-6/JAK/STAT pathway and the nuclear factor-κB pathway, and the possible involvement of the inflammasome, the exact mechanisms underlying the development of HCC in chronic liver disease remain obscure.[2] Furthermore, a small fraction of HCC has been known to occur in patients with a seemingly intact liver. Such non-cirrhotic HCC may share several characteristics with hepatocellular adenoma,[3] which has been shown to undergo malignant transformation with an overall frequency of 4.2%.[4] There might be different tumorigenic mechanisms between tumors associated with chronic injury or cirrhosis and those that develop in seemingly intact livers.

A variety of mouse models of hepatocarcinogenesis have been used to elucidate the mechanisms underlying the development of HCC. The most widely used is the diethylnitrosamine (DEN)-induced model,[5] in which hepatocellular adenoma and HCC develop in an intact, non-cirrhotic liver. Several liver tumor-prone transgenic mouse lines have also been generated by the introduction of HBsAg and HBx,[6] SV40 large T antigen, a secretable form of epidermal growth factor (EGF),[7] or oncogenes such as E2F-1, c-Myc, and transforming growth factor-α.[8] In these models, liver tumors also developed in non-cirrhotic livers; thus, the results that were obtained need to be interpreted cautiously when they are extrapolated for understanding the pathogenesis of human HCC that develops in fibrotic or cirrhotic backgrounds. Conversely, long-standing centrilobular injury inflicted by the chronic administration of CCl_4 or thioacetamide (TAA) in adult mice can induce liver tumors in a fully established cirrhotic background.[9,10]

In the present study, to gain insights into the tumorigenic mechanisms in cirrhotic and non-cirrhotic conditions, we compared the mRNA expression profiles of mouse liver tumors induced by the repeated injection of CCl_4 (cirrhotic protocol) or a single DEN injection when the mice were 2 weeks old (non-cirrhotic protocol) using a cDNA microarray and quantitative RT-PCR (RT-qPCR). We identified several genes whose mRNA expression was increased predominantly in either CCl_4-induced or DEN-induced liver tumors as well as genes that were increased comparably in both. We further examined the mRNA expression of the identified genes, most of which were also highly expressed in the fetal/neonatal liver, in other mouse liver tumors induced under cirrhotic and non-cirrhotic conditions.

Materials and Methods

Animals. C3H/HeNCr1Cr1j (C3H) and C57BL/6J (C57) mice were purchased from Charles River Laboratories Japan (Yokohama, Japan). C3H × C57 F1 offspring were generated by breeding male C3H and female C57 mice. The mice were killed under deep anesthesia, and the livers were removed for further examination. The protocols used for animal experimentation were approved by the Animal Research Committee, Asahikawa Medical University (Asahikawa, Japan), and all animal experiments adhered to the criteria outlined in the Guide for the Care and Use of Laboratory Animals prepared by the National Academy of Sciences (8th edn, 2011).

Mouse liver tumor models. Male C3H × C57 F1 or C57 mice (8–10-weeks old) were treated with CCl_4 (Kanto Chemical, Tokyo, Japan) three times per week (1 mL/kg, s.c.; 1:5 dilution in olive oil) for 24 weeks to induce liver cirrhosis and subsequent tumor formation. Male C3H × C57 F1 mice were also treated with TAA (Sigma-Aldrich, St. Louis, MO, USA) (0.03% in drinking water) for 30 weeks to generate another cirrhotic model of liver tumors.

To induce liver tumors in a non-cirrhotic background, C3H × C57 F1 mice were treated with a necrotizing dose of DEN (5 mg/kg, i.p.) at 2 weeks after birth and killed after 44 weeks. As another non-cirrhotic model, liver tumors that had spontaneously developed in C3H mice aged 13–15 months were analyzed.[11]

cDNA microarray analysis. Total RNA was prepared from snap-frozen liver tissues using the RNeasy Mini Kit (Qiagen, Chatsworth, CA). Samples of CCl_4-induced liver tumors (a mixture of five independent large tumors), DEN-induced liver tumors (a mixture of five independent large tumors), CCl_4-induced cirrhotic liver tissues (non-tumorous tissues of livers harboring tumors, a mixture of five tissues from five mice), and control liver tissue (olive oil-treated; a mixture of two tissues from two mice) were analyzed and compared by one-color microarrays (3D-Gene Microarray; Toray, Tokyo, Japan). After background subtraction, the raw microarray data were normalized using a standard global normalization technique, and the signal intensities were calculated as the fold changes of expression values. The data of differentially expressed genes that were significantly changed (>4-fold, compared with control) were subjected to Z-score transformation and loaded in a centroid-linkage hierarchical clustering assay using a Pearson correlation (uncentered) similarity metric with Cluster 3.0. Then, the Java TreeView software (http://jtreeview.sourceforge.net/) was applied to reveal the hierarchical gene groups

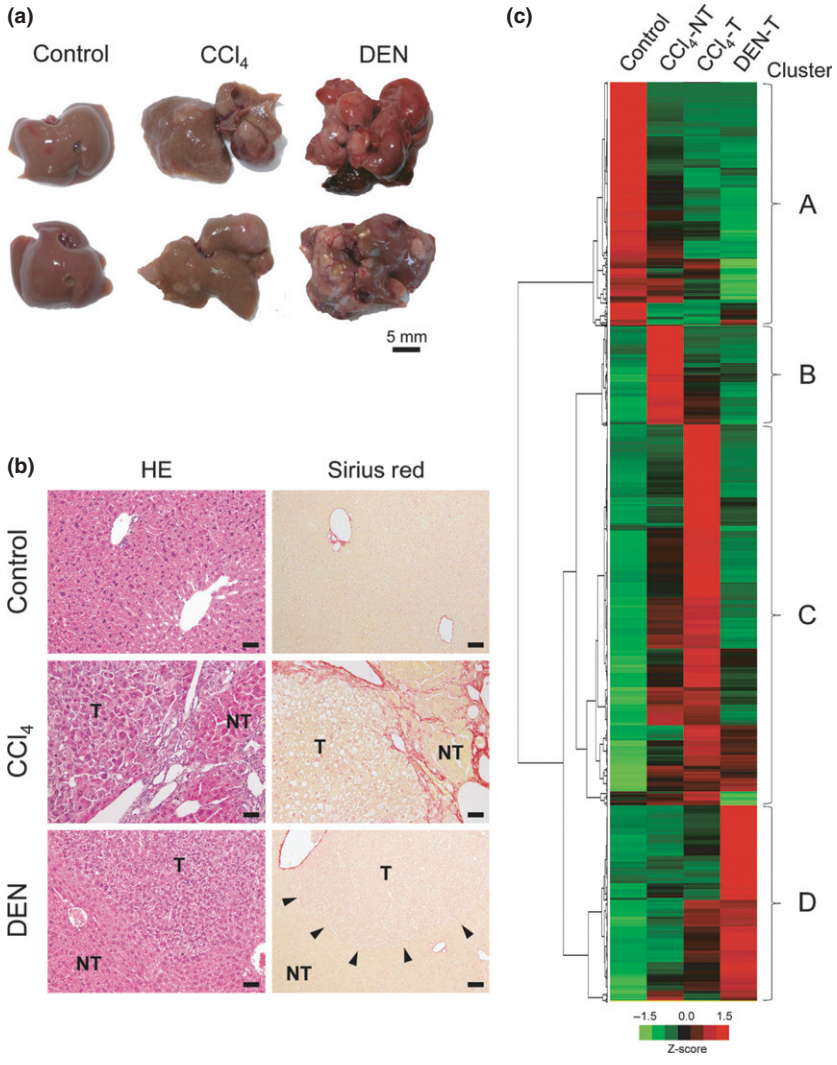

Fig. 1. Identification of differentially expressed genes in mouse liver tumors induced in cirrhotic and non-cirrhotic models. (a) Gross appearance of livers from control (olive oil-treated, 32-week-old), CCl_4-treated (32-week-old), and diethylnitrosamine (DEN)-treated (46-week-old) mice. (b) Histology of the liver tissues from control, CCl_4-treated, and DEN-treated mice; HE and Sirius Red staining. NT, non-tumor; T, tumor. Arrowheads indicate the boundary of a DEN-induced tumor. Scale bar = 50 μm. (c) cDNA microarray analysis showing genetic clusters (A–D) of differentially expressed genes in control liver tissues (olive oil-treated), CCl_4-induced cirrhotic tissues (CCl_4-NT), CCl_4-induced tumors (CCl_4-T), and DEN-induced tumors (DEN-T).

Table 1. Top 10 highly expressed genes in CCl_4-induced tumors in genetic cluster C

Gene	Fold change *vs* control (log2)		
	Cirrhosis (CCl_4-NT)	CCl_4 tumor (CCl_4-T)	DEN tumor (DEN-T)
Insulin-like growth factor 2 (*Igf2*)	6.97	9.70	3.06
Lymphocyte antigen 6 complex, locus D (*Ly6d*)	6.46	8.33	6.55
Carboxypeptidase E (*Cpe*)	3.77	8.21	7.68
H19 fetal liver mRNA (*H19*)	5.48	8.13	6.47
Secretory leukocyte peptidase inhibitor (*Slpi*)	3.52	6.92	6.35
Keratin 20 (*Krt20*)	4.70	6.83	4.41
Stearoyl-Coenzyme A desaturase 2 (*Scd2*)	4.86	6.51	5.65
Topoisomerase (DNA) II alpha (*Top2a*)	5.03	6.18	3.89
Calcium and integrin binding family member 3 (*Cib3*)	3.76	6.15	3.58
Carbonyl reductase 3 (*Cbr3*)	2.55	6.04	2.35

DEN-T, diethylnitrosamine-induced tumor; CCl_4-NT, CCl_4-induced cirrhotic tissue (non-tumor); CCl_4-T, CCl_4-induced tumor.

Table 2. Top 10 highly expressed genes in diethylnitrosamine (DEN)-induced tumors in genetic cluster D

Gene	Fold change *vs* control (log2)		
	Cirrhosis (CCl_4-NT)	CCl_4 tumor (CCl_4-T)	DEN tumor (DEN-T)
Glypican 3 (*Gpc3*)	2.63	6.06	8.62
Aldo-keto reductase family 1, member C18 (*Akr1c18*)	3.26	6.44	8.57
Flavin containing monooxygenase 3 (*Fmo3*)	0.60	1.90	7.33
ATP-binding cassette, sub-family D, member 2 (*Abcd2*)	3.89	4.90	7.32
Tetraspanin 8 (*Tspan8*)	3.92	6.29	7.23
Alpha fetoprotein (*Afp*)	4.19	4.47	7.11
Trefoil factor 3, intestinal (*Tff3*)	0.91	6.30	6.98
Serine peptidase inhibitor, Kazal type 3 (*Spink3*)	6.68	6.22	6.92
Patatin-like phospholipase domain containing 5 (*Pnpla5*)	1.94	3.88	6.53
Cyclin-dependent kinase inhibitor 2B (*Cdkn2b*)	1.84	4.73	5.96

DEN-T, DEN-induced tumor; CCl_4-NT, CCl_4-induced cirrhotic tissue (non-tumor); CCl_4-T, CCl_4-induced tumor.

among the four samples. The Z-score was cropped to −1.5 to +1.5 when generating a two-color heat map.

Quantitative RT-PCR. Total RNA were extracted from frozen liver tissues and subjected to RT-qPCR analyses. Quantitative RT-PCR was carried out using the $^{\Delta\Delta}C_t$ method with FastStart Universal SYBR Green Master Mix (Roche Diagnostics, Mannheim, Germany). Each reaction was carried out in duplicate, and the mRNA levels were normalized to *Gapdh*. The sequences of the specific primers are listed in Table S1. Two-dimensional hierarchal clustering of tumor-associated genes was carried out using Z-score-normalized data. The Z-score was cropped to −2.0 to +2.0 when generating a two-color heat map.

Microscopic examination, immunohistochemistry, and *in situ* hybridization. The livers were fixed in phosphate-buffered 10% formalin for 24 h, and paraffin sections were then prepared. Immunohistochemical staining was carried out with the EnVision/HRP system (Dako, Carpinteria, CA, USA) on deparaffinized sections treated with Target Retrieval Solution (Dako). The antibodies used were as follows: anti-insulin-like growth factor 2 (IGF2) (ab9574; Abcam, Cambridge, UK), anti-α-fetoprotein (AFP) (14550-1-AP, for mouse tissues; Proteintech Group, Chicago, IL, USA), anti-AFP (A0008, for human tissues; Dako), and anti-trefoil factor 3 (TFF3) (Abbiotec, San Diego, CA, USA). 3,3′-Diaminobenzidine tetrahydrochloride (Vector Laboratories, Burlingame, CA, USA) was used for signal detection. For the detection of the TFF3 peptide, we applied signal amplification using the TSA Plus DIG Kit (PerkinElmer, Waltham, MA, USA). *In situ* hybridization for non-coding *H19* mRNA was carried out on deparaffinized sections using the mouse H19 QuantiGene ViewRNA Probe Set (VB6-16706; Affymetrix, Santa Clara, CA, USA) and the QuantiGene ViewRNA ISH Tissue Assay Kit (Affymetrix).

Human liver samples. The retrospective analysis of surgical specimens was approved by the internal review board of Asahikawa Medical University. A total of 33 HCC samples from patients who had curative hepatectomy and five intact liver tissues surrounding the resected cavernous hemangiomas were collected. Among the HCC samples, nine cases were devoid of any detectable fibrosis or inflammation in the non-tumorous liver parenchyma, whereas the rest showed various degrees of liver fibrosis (fibrous expansion of the portal tract, bridging fibrosis, and cirrhosis).

Statistical analysis. Unpaired two-tailed *t*-tests or one-way ANOVA were used to compare differences in gene expression. The correlation between Ki-67 staining and the mRNA levels of genes was assessed by Spearman's correlation coefficients. Fisher's exact test was used to evaluate the differences in expression of various proteins in HCC samples between the groups with and without liver fibrosis.

Results

cDNA microarray analyses of differentially expressed genes in CCl_4-induced and DEN-induced mouse liver tumors. Following repeated injections of CCl_4, numerous relatively small tumors appeared in the markedly fibrotic and cirrhotic liver parenchyma, whereas in the DEN model, multiple large tumors developed in the non-cirrhotic background (Fig. 1a). Histologically, both CCl_4- and DEN-induced tumors were hepatocyte tumors, with features of hepatocellular adenoma and well-differentiated HCC (Fig. 1b). The surrounding non-tumorous liver tissues were cirrhotic in the CCl_4 model but were almost normal and non-cirrhotic in the DEN model, as revealed by Sirius Red staining (Fig. 1b). The cDNA microarray analysis identified 1028 differentially expressed genes in the intact liver tissues (control), CCl_4-induced cirrhotic tissues (non-tumor, NT) (CCl_4-NT), CCl_4-induced tumors (CCl_4-T), and DEN-induced tumors (DEN-T) across genetic clusters A–D (Fig. 1c). Several genes, such as *S100g*, *Cyp4a14*, and *Mmp7*, were selectively activated in cirrhotic tissues (CCl_4-NT), while the expression of others, such as *Fabp6* and *Plat*, was increased in both CCl_4-NT and CCl_4-T (Table S2). We focused on the tumor-associated genes that were highly

expressed in either CCl_4- or DEN-induced tumors (Tables 1, 2).

Validation of mRNA expression profiles by RT-qPCR and *in situ* detection of IGF2, *H19* mRNA, TFF3, and AFP in tumors. The levels and patterns of mRNA expression of the identified genes were validated by RT-qPCR analyses. The mRNA expression of *H19*, *Igf2*, *Cbr3*, and *Krt20* was predominantly increased in CCl_4-induced tumors (more than 4-fold that observed in DEN-induced tumors; referred to as CCl_4-associated); that of *Tff3*, *Akr1c18*, *Gpc3*, *Afp*, and *Abcd2* was predominantly increased in DEN-induced tumors (more than 4-fold over that in CCl_4-induced tumors; referred to as DEN-associated), and that of *Ly6d*, *Slpi*, *Spink 3*, *Scd2*, and *Cpe* was increased at comparable levels in CCl_4- and DEN-induced tumors (referred to as Common) (Fig. 2a). The changes in mRNA expression observed in the remaining genes (*Cib3*, *Top2a*, *Cdkn2b*, *Pnpla5*, and *Tspan8*) in the tumors were not statistically significant (Fig. S1).

Among the changes in mRNA expression associated with CCl_4-induced tumors, an increase in *Igf2* and *H19* mRNA was the most specific and was found in approximately half of the tumors. In addition, the magnitude of the induction of *Tff3* mRNA, especially in DEN-tumors, was very impressive. To confirm the protein expression of IGF2 and TFF3 and the mRNA expression of *H19* in liver tumors, we carried out immunohistochemistry for IGF2 and TFF3 and *in situ* hybridization for *H19*. The expression of AFP, a prototype oncofetal marker for HCC, was also examined. Although all of these were negative in adult liver tissues, IGF2 was positive in approximately half of CCl_4-induced tumors but completely negative in DEN-induced tumors (Fig. 2b). *H19* mRNA was strongly expressed in some CCl_4-induced tumors (Fig. 2b). Diethylnitrosamine-induced tumors also expressed *H19* mRNA, but its levels were generally low (Fig. 2b). Although TFF3 was detected in both types of tumors, DEN-induced tumors tended to show stronger staining (Fig. 2b). α-Fetoprotein was strongly positive in DEN-induced tumors, whereas CCl_4-induced tumors were negative or contained scattered positive cells (Fig. 2b).

Relationship between proliferative activity of tumor cells and mRNA expression levels of tumor-associated genes. We next examined whether the mRNA expression of the tumor-associated genes correlated with tumor cell proliferation, as estimated by Ki-67 immunohistochemistry. In the CCl_4 model, the expression levels of *Cbr3* and *Tff3* were correlated with the proliferative activity of the tumor cells (Fig. 3). Although *Igf2*

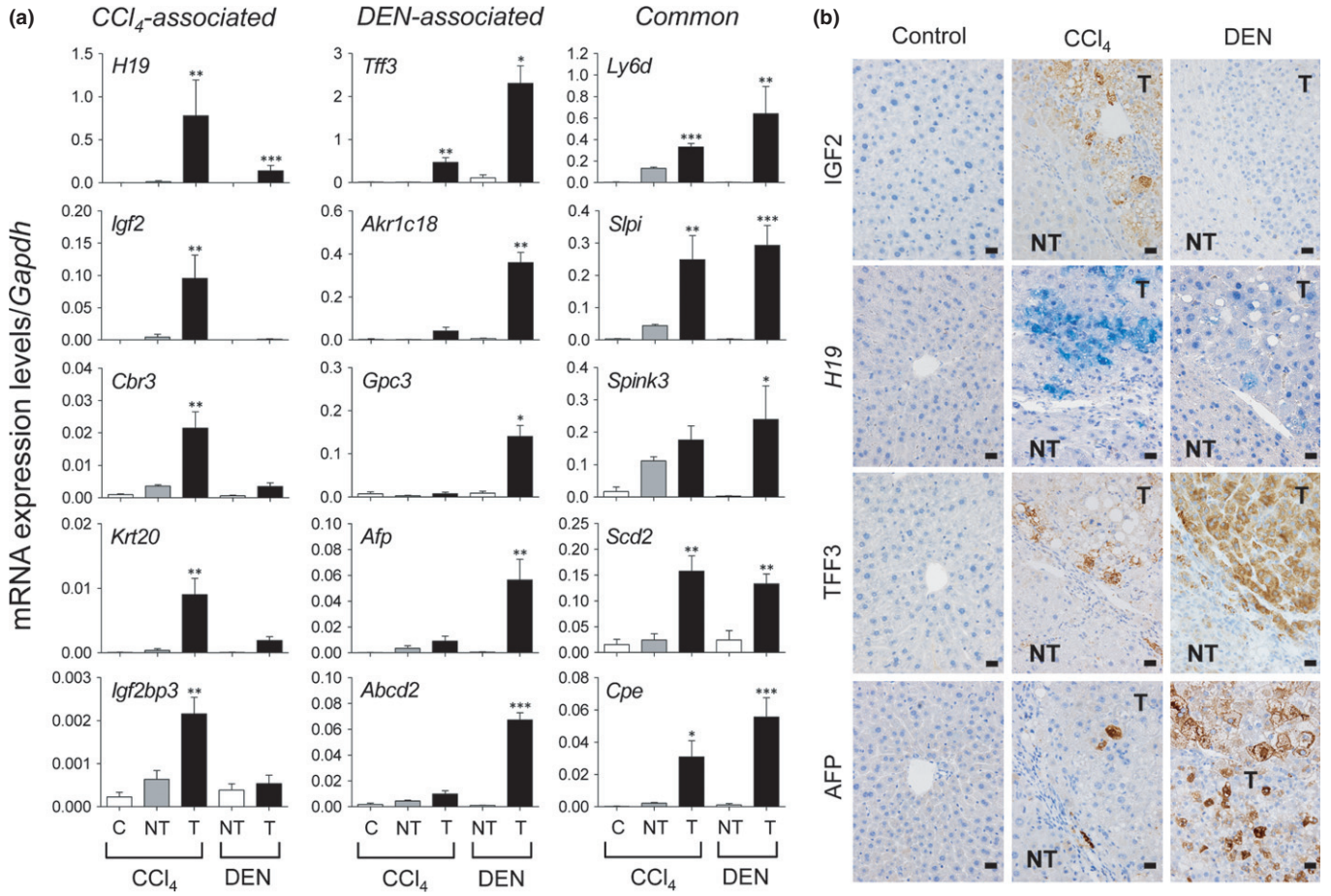

Fig. 2. Differential expression of mRNA and their products in CCl_4-induced and diethylnitrosamine (DEN)-induced liver tumors. (a) Quantitative RT-PCR analyses of mRNA expression of 15 tumor-associated genes. The genes preferentially expressed in CCl_4-induced tumors and DEN-induced tumors are designated "CCl_4-associated" and "DEN-associated," respectively, and those comparatively expressed in CCl_4-induced and DEN-induced tumors are designated "Common." Each value is expressed as the mean ± SEM. The ages of the mice at analyses were 32–34 weeks and 46 weeks in the CCl_4-induced and DEN-induced models, respectively. The number of samples in each group was 5, 12, 15, 6, and 13 for CCl_4 control (olive oil, C), CCl_4-induced cirrhosis (NT), CCl_4-induced tumors (T), DEN control (NT), and DEN-induced tumors (T), respectively. $^*P < 0.05$, $^{**}P < 0.01$, $^{***}P < 0.001$ *versus* control; one-way factorial ANOVA. (b) *In situ* detection of insulin-like growth factor 2 (IGF2), *H19* mRNA, trefoil factor 3 (TFF3), and α-fetoprotein (AFP) in CCl_4-induced and DEN-induced tumors. Immunohistochemistry for IGF2, TFF3, and AFP and *in situ* hybridization for *H19* mRNA. NT, non-tumor; T, tumor. Scale bar = 20 μm.

encodes IGF2, which has been shown to play important roles in cell growth, *Igf2* mRNA expression was not significantly correlated with tumor cell proliferation, similar to other genes (Figs 3,S2). In the DEN model, the expression of none of the genes analyzed was related to the proliferative activity of the tumor cells (Figs 3,S2).

Fetal or neonatal expression of tumor-associated genes. Because the identified tumor-associated genes included well-known oncofetal genes, such as *Igf2*, *H19*, *Gpc3*, and *Afp*, we examined their mRNA expression during fetal and neonatal periods. Our results clearly showed that all of these genes, with the exceptions of *Cbr3* and *Cpe*, were highly expressed in either the fetal or neonatal periods (Fig. 4a), indicating that the differential activation of fetal/neonatal gene expression occurs in CCl_4- and DEN-induced liver tumors. As expected, the protein expression of IGF2 and TFF3 and the mRNA expression of *H19* were detected in hepatoblasts/hepatocytes during the fetal or neonatal period (Fig. 4b).

Comparison with other cirrhotic and non-cirrhotic liver tumor models. Next, we examined whether similar differential activation could also be observed in other liver tumor models. Thioacetamide-induced selective centrilobular injuries and chronic TAA administration resulted in multiple liver tumors (hepatocellular adenoma or well differentiated HCC), which were associated with marked cirrhosis in the surrounding liver (Fig. 5a). In TAA-induced tumors, there were increases in the expression of *Igf2* mRNA and *Krt20* mRNA, with a tendency for increased mRNA expression of *H19* and *Igf2bp3* (Fig. 5b). In contrast, the mRNA expression of *Akr1c18*, *Gpc3*, and *Afp*, which was highly characteristic of DEN-induced tumors, was not observed in TAA-induced tumors, although there was an increase in *Abcd2* mRNA (Fig. 5b). In spontaneously formed liver tumors (well to moderately differentiated HCC) in the intact livers of aged C3H mice, there was no increase in the mRNA expression of the genes that were selectively increased in CCl_4-induced tumors, but the mRNA expression of *Tff3*, *Akr1c18*, *Afp*, and *Abcd2* was significantly increased (Fig. 5b). The mRNA expression of all the "common" genes was increased in TAA-induced tumors, whereas that of *Spink3*, *Scd2*, and *Cpe* was lacking in the spontaneously formed tumors (Fig. 5b).

Two-dimensional hierarchical cluster analysis of tumor-associated genes in cirrhotic and non-cirrhotic models. The mRNA expression data of the 15 tumor-associated genes in the four different liver tumor models (CCl_4-induced, DEN-induced, TAA-induced, spontaneous) were subjected to unsupervised 2-D hierarchical cluster analysis (Fig. 6). Interestingly, the mRNA expression profiles of the 15 genes almost clearly segregated control liver tissues, cirrhotic tissues, and tumors that had developed in the cirrhotic and non-cirrhotic backgrounds. Furthermore, there were several clusters of between two and four transcripts, which characterized tumors that had developed in the cirrhotic background (*H19*, *Igf2*, and *Igf2bp3*), in the non-cirrhotic background (*Tff3*, *Akr1c18*, *Abcd2*, and *Gpc3*), and in either background (*Scd2* and *Slpi*; *Cpe* and *Ly6d*).

Selective activation of *IGF2* and its related genes in CCl_4- or TAA-induced tumors. There was a significant positive correlation between the mRNA expression levels of *Igf2* and *H19* (Fig. 7a), which are known to be adjacently located in the genome and are regulated through reciprocal imprinting and a common enhancer.[12,13] The mRNA expression of *Igf2bp3*, whose product is functionally correlated with *Igf2* mRNA and *H19* mRNA,[14] was also increased in CCl_4-induced tumors (Fig. 2). The expression of *Igf2bp3* mRNA was significantly higher in tumors with substantial levels of *Igf2* mRNA expression (*Igf2/Gapdh* $\geq$0.01) compared with those that showed very low or no *Igf2* mRNA expression (*Igf2/Gapdh* <0.01) (Fig. 7b). Similar findings were obtained with TAA-induced tumors (Fig. 7).

Expression of IGF2, TFF3, and AFP in human HCC with or without liver fibrosis. The above experiments indicated that IGF2

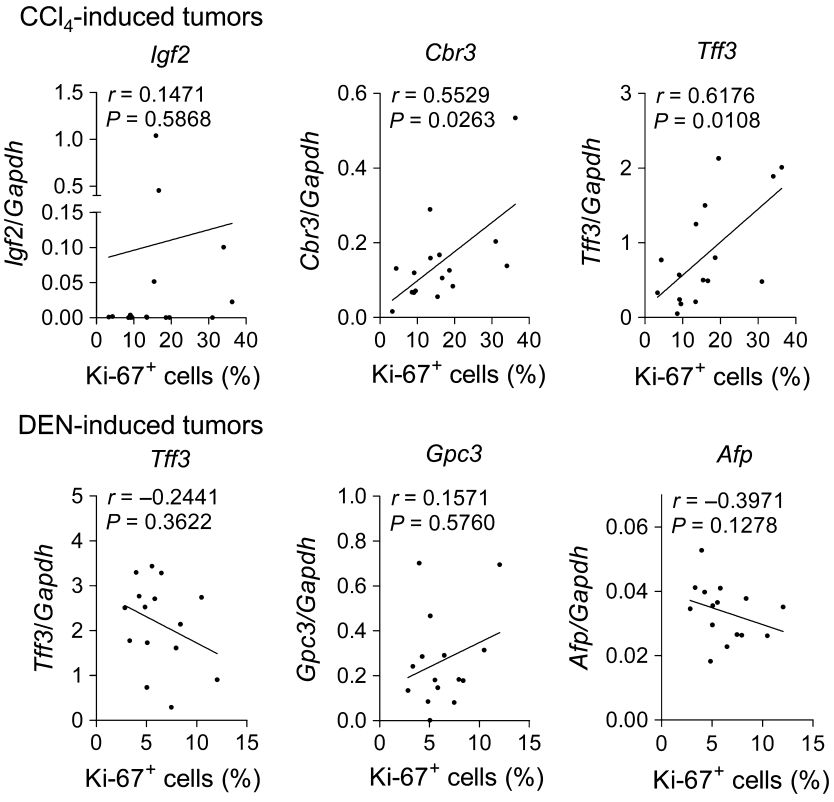

Fig. 3. Relationship between mRNA expression of tumor-associated genes and tumor cell proliferation. Scatter plots of mRNA expression levels of selected tumor-associated genes and Ki-67 labeling index (%) in CCl_4-induced tumors (n = 16) and diethylnitrosamine (DEN)-induced tumors (n = 15). Spearman correlation coefficients were used to test the association of mRNA expression and tumor cell proliferation.

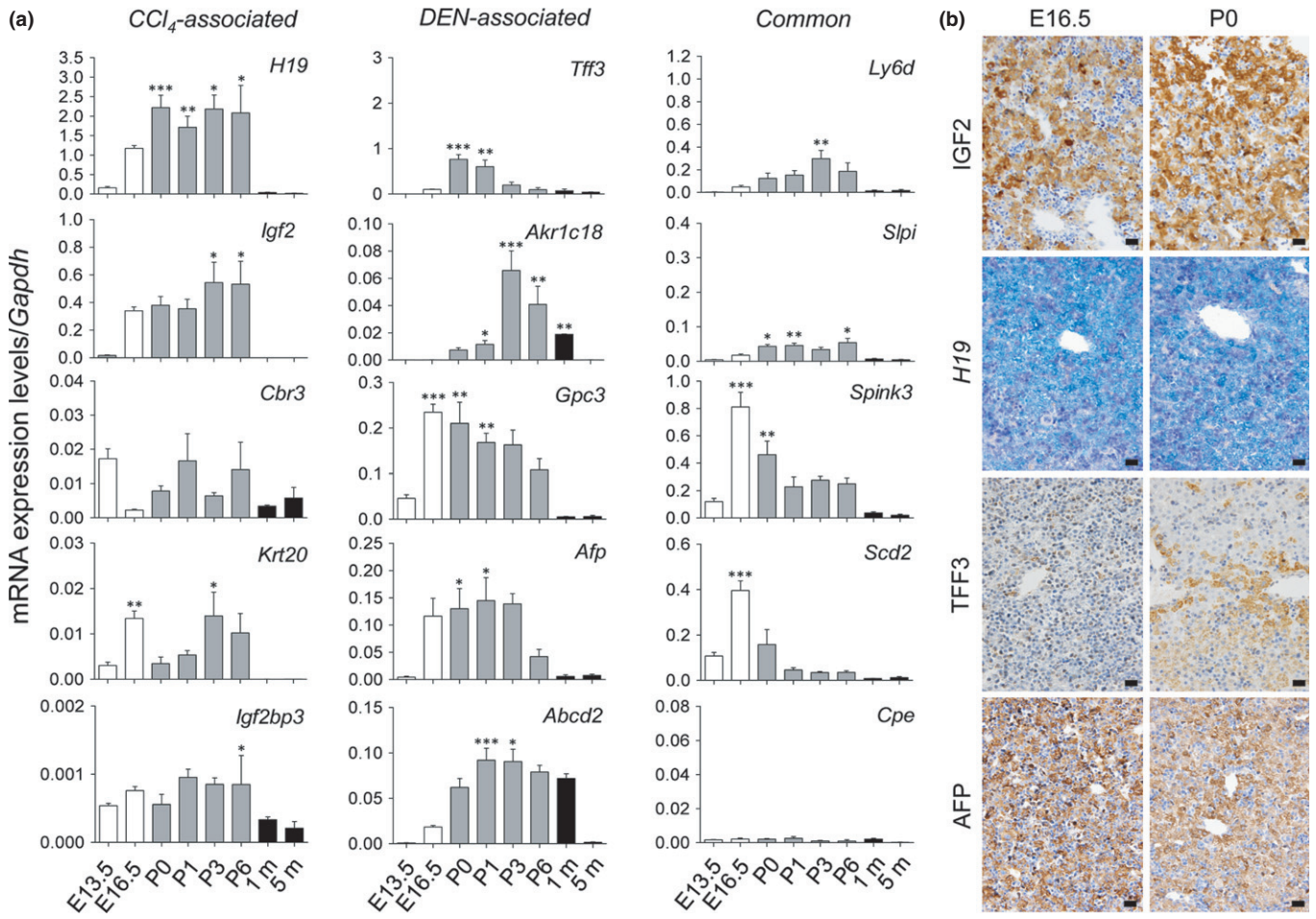

Fig. 4. Fetal/neonatal activation of tumor-associated genes and their products. (a) Quantitative RT-PCR analyses of mRNA expression of tumor-associated genes during fetal/neonatal periods. Each value is expressed as the mean ± SEM. The number of samples in each group was 3, 5, 7, 10, 4, 4, 4, and 7 for E13.5, E16.5, P0 (immediately after birth), P1 (1 day after birth), P3 (3 days after birth), P6 (6 days after birth), 1 m (1 month old), and 5 m (5 months old), respectively. $^{*}P < 0.05$, $^{**}P < 0.01$, $^{***}P < 0.001$ *versus* control (5 m); one-way factorial ANOVA. (b) *In situ* detection of insulin-like growth factor 2 (IGF2), *H19* mRNA, trefoil factor 3 (TFF3), and α-fetoprotein (AFP) in developing livers. Immunohistochemistry for IGF2, TFF3, and AFP and *in situ* hybridization for *H19* mRNA in fetal (E16.5) and neonatal (P0) livers. Scale bar = 20 μm.

expression showed significant discrimination ability for mouse liver tumors developed in cirrhotic and non-cirrhotic backgrounds. We examined IGF2 expression in human HCC developed with seemingly intact (non-fibrotic) livers or fibrotic livers. Immunohistochemically, tumor cells stained positive for either IGF2, TFF3, or AFP were found in several HCC cases, whereas these were negative in the surrounding liver parenchyma (Fig. 8a). Clusters of IGF2-positive tumor cells were present in 11.1% and 54.2% of HCC developed with non-fibrotic livers ($n = 9$) and those developed with fibrotic livers ($n = 24$), respectively (Fig. 8b). This difference was statistically significant ($P = 0.0466$, Fisher's exact test). In contrast, there were no significant differences in the expression of TFF3 or AFP in HCC developed under these different conditions (Fig. 8b).

Discussion

We identified genes whose mRNA expression was increased in mouse liver tumors induced in cirrhotic and non-cirrhotic conditions. Based on gene expression clustering of these genes, we could distinguish tumors arising in the two different backgrounds, indicating the presence of genes that are differentially expressed during the tumorigenic course. Interestingly, most of the tumor-associated genes were also activated in the fetal/neonatal periods. The activation of these genes, including well established oncofetal genes (e.g., *Afp*, *Igf2*, *H19*, and *Gpc3*),[15–17] occurred in the late fetal period (E16.5) and persisted during the postnatal period. This finding indicates that the mRNA expression of these genes in the liver tumors might not reflect the simple dedifferentiation of transformed hepatocytes into immature hepatoblasts. Although the significance of the reactivation of fetal/neonatal genes in mouse liver tumors is unclear, our study shows that transformed hepatocytes might use the cellular system that is active during the fetal/neonatal periods, when the most robust physiological proliferation of hepatocytes occur.[18]

Tff3 mRNA and its product, an intestinal polypeptide, TFF3, were highly expressed in mouse liver tumors, particularly in those induced by DEN in C3H × C57 F1 and those that developed spontaneously in C3H mice. The TFF3 polypeptide was also detected in human HCC arising in either fibrotic or non-fibrotic liver. It has been reported that *Tff3* mRNA expression is increased in spontaneous liver tumors in tumor-prone PWK mice and those that develop in SV40 T antigen transgenic mice, as well as in human HCC.[19] Marked increases in *Tff3*

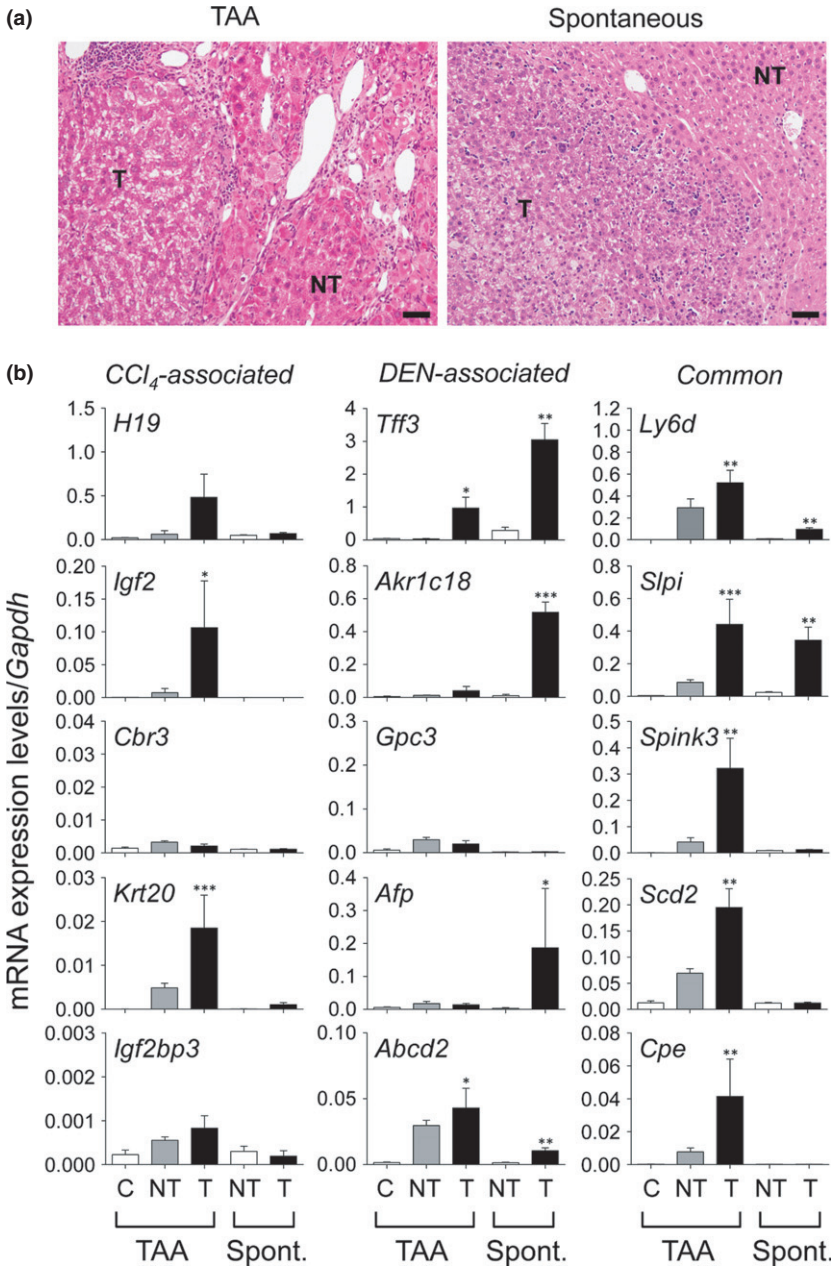

Fig. 5. Differential gene expression in thioacetamide (TAA)-induced liver tumors and spontaneously developed liver tumors in mice. (a) Histology of liver tissues from TAA-induced and spontaneous tumors. The ages of mice at analyses were 38–40 weeks and 13–15 months in the TAA-induced model and spontaneous model, respectively. HE staining. NT, non-tumor; T, tumor. Scale bar = 50 μm. (b) Quantitative RT-PCR analyses of mRNA expression of 15 tumor-associated genes in TAA-induced and spontaneous (Spont.) tumors. Each value is expressed as the mean ± SEM. The number of samples in each group was 7, 6, 9, 4, and 3 for the TAA control (C), TAA-induced cirrhosis (NT), TAA-induced tumors (T), control C3H mouse liver (NT), and spontaneous tumors (T) in C3H mice, respectively. $*P < 0.05$, $**P < 0.01$, $***P < 0.001$ *versus* control; one-way factorial ANOVA.

mRNA have also been found in liver tumors that developed in *HBx* transgenic mice[20] and those that developed in secretable EGF-expressing transgenic mice.[7] The expression of *Tff3* mRNA is governed by several transcription factors, including hepatocyte nuclear factor 3 and nuclear factor-κB, and by DNA methylation of its promoter region. Specifically, promoter hypomethylation has been found in mouse liver tumors and human HCC.[19] Although TFF3 is highly expressed in goblet cells in the intestinal mucosa and has been suggested to be important in the processes of mucosal repair,[21] its role in hepatocarcinogenesis is currently obscure. However, *Tff3* mRNA or TFF3 polypeptide may serve as useful biomarkers due to their high specificity to liver tumors.

Our study revealed that *Igf2* and its related genes, *H19* and *Igf2bp3*, were selectively activated in approximately half of the mouse liver tumors induced under cirrhotic, but not non-cirrhotic, conditions. The expression of *Igf2bp3* mRNA was significantly higher in the *Igf2*-expressing tumors induced by CCl_4, suggesting their functional correlation. *Igf2* and *H19*, which is located immediately downstream of *Igf2*, are reciprocally imprinted through the hypomethylation and methylation of the differentially methylated region on the maternal allele and paternal allele, respectively, and their expression is dependent on the two endoderm-specific enhancers that lie 3′ of *H19*.[12] Although we do not know whether the loss of imprinting or altered methylation states of this gene cluster might contribute to their activation, a highly significant correlation between the *Igf2* mRNA and *H19* mRNA levels in the tumors suggests that their transcriptional activation is mediated by common enhancers.[13] Increased mRNA expression of *IGF2* and *H19*, as well as a significant correlation of their mRNA expression levels, have been shown in human HCC.[22–25] However, following a partial hepatectomy in rodents, whereas *H19* mRNA is markedly induced, *Igf2* mRNA expression is

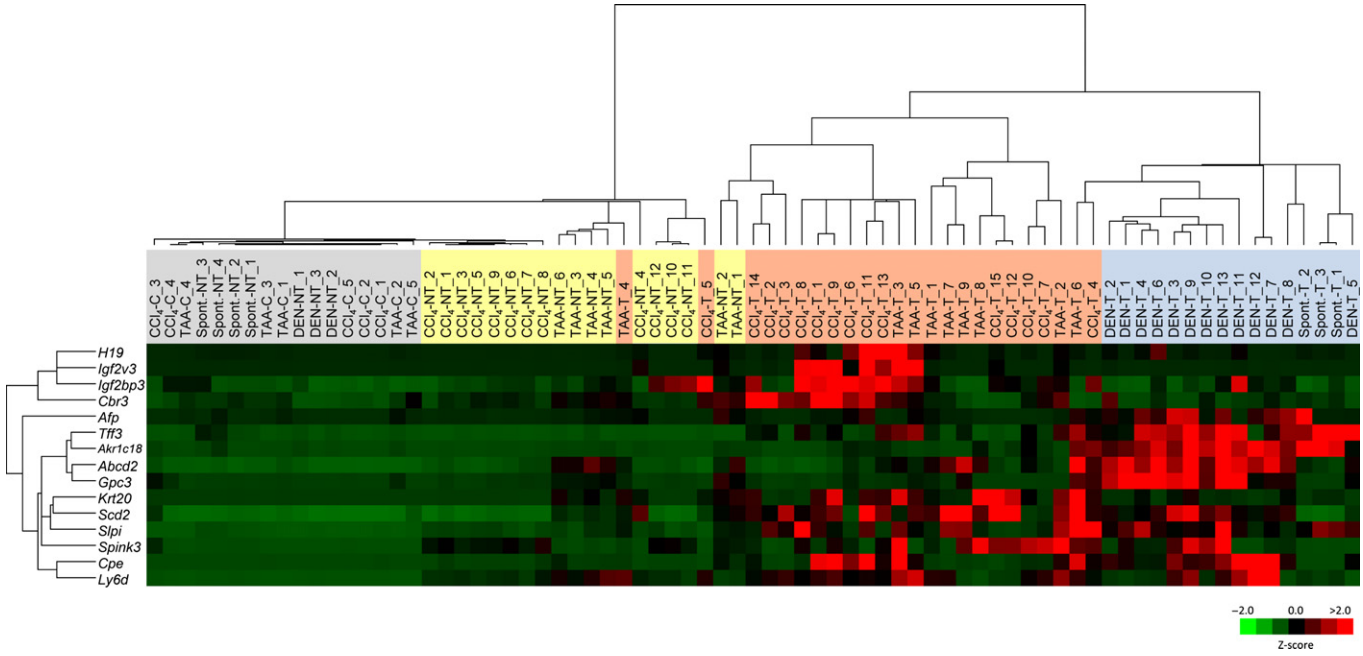

Fig. 6. Heatmap of 2-D hierarchical clustering of mRNA expression of 15 tumor-associated genes in four different liver tumor models: CCl_4-induced, diethylnitrosamine (DEN)-induced, thioacetamide (TAA)-induced, and spontaneous.

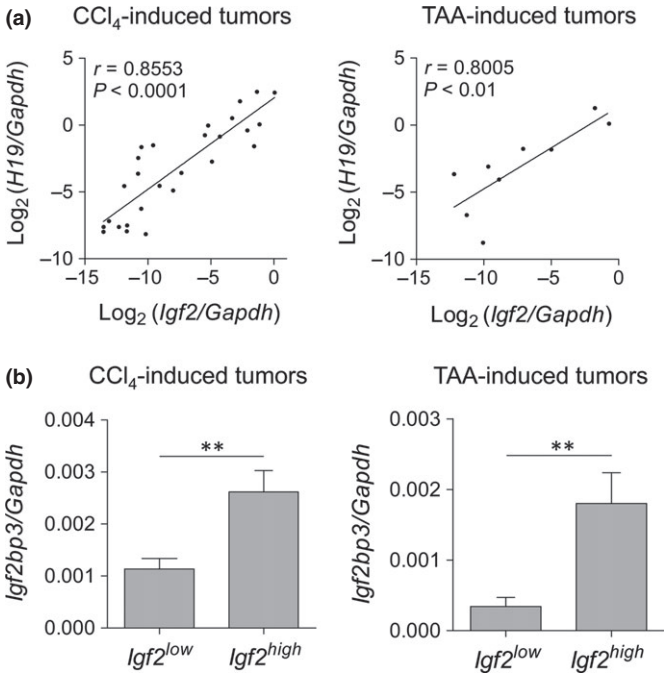

Fig. 7. Association between mRNA expression of *Igf2* and its related genes in CCl_4- and thioacetamide (TAA)-induced tumors. (a) Scatter plot showing a positive correlation between the mRNA expression of *Igf2* and *H19* in CCl_4-induced tumors (n = 27) and TAA-induced tumors (n = 9). Spearman's correlation coefficient was used to test the correlation between the expression of the transcripts. (b) *Igf2bp3* mRNA expression in tumors with substantial *Igf2* mRNA expression (*Igf2*^{high}, *Igf2*/*Gapdh* ≥0.01; CCl_4-induced tumors, n = 12; TAA-induced tumors, n = 3) and very low or no *Igf2* mRNA expression (*Igf2*^{low}, *Igf2*/*Gapdh* <0.01; CCl_4-induced tumors, n = 19; TAA-induced tumors, n = 6). $^{**}P < 0.01$; unpaired two-tailed t-test.

not activated,[26] indicating a striking contrast between non-transformed and transformed hepatocytes.

Our analysis of human liver samples showed the lower frequency of IGF2 positivity in tumor cells in cases of HCC arising in almost intact liver, compared with those with various degrees of fibrosis. Interestingly, in an attempt of transcriptional classification of human HCC into six subgroups, an identified subgroup (G1) was characterized by the reactivation of *IGF2* gene expression, as well as the association with HBV infection.[25] Although further confirmation is needed in view of the small number of cases analyzed, our data suggest the possible involvement of the IGF2 signaling in human hepatocarcinogenesis that is associated with chronic liver injury and fibrosis.

Although the exact mechanisms of HCC development in chronically injured and fibrotic liver are not clear, it is probable that the continued stimuli for hepatocyte regeneration following liver injury may play important roles in this process.[27] Repeated hepatocyte injury promotes hepatic tumorigenesis in hepatitis C virus transgenic mice,[28] possibly through excessive EGF receptor and/or c-Met signaling activities.[27] While our study elucidated the close association between the activation of *Igf2* gene expression and the cirrhotic hepatocarcinogenesis, reactivation of *Igf2* gene expression in liver tumors has been shown in the absence of liver injury in various experimental models with enhanced hepatocyte proliferation in whole livers, such as *HBx* and *SV40 T Ag* transgenic mice.[20,29,30] In *SV40 T Ag* transgenic mice, as well as in HBV presurface gene (*preS1* and *preS2*) transgenic mice, in which benign and malignant hepatocytic nodules appear following perpetual hepatocyte apoptosis and regeneration, IGF2 reactivation has been found to be associated with late progression steps toward HCC.[30] Furthermore, in secretable EGF-expressing transgenic mice, there is a switch from the initial

(a)

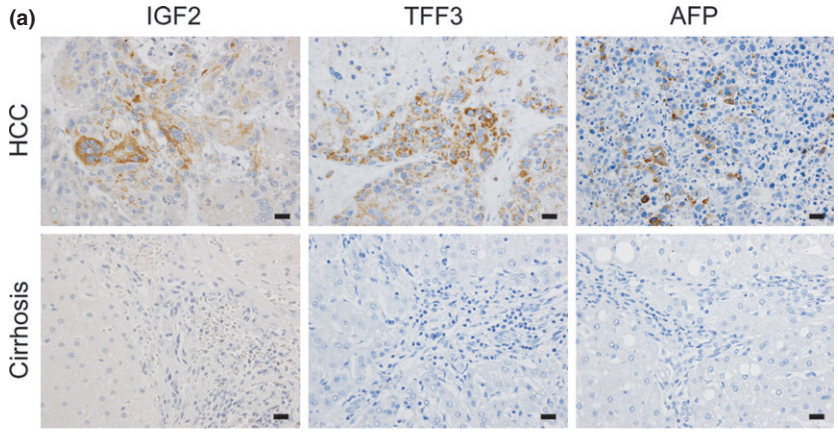

(b)

	Surrounding liver tissues				*P*-value (Fisher's exact test)
	Non-fibrotic (*n* = 9)		Fibrotic (*n* = 24)		
	+	–	+	–	
IGF2	1 (11.1%)	8 (88.9%)	13 (54.2%)	11 (45.8%)	0.0466
TFF3	4 (44.4%)	5 (55.6%)	7 (29.2%)	17 (70.8%)	0.1460
AFP	3 (33.3%)	6 (66.7%)	6 (25.0%)	18 (75%)	0.2753

Fig. 8. Expression of insulin-like growth factor 2 (IGF2), trefoil factor 3 (TFF3), and α-fetoprotein (AFP) in human hepatocellular carcinoma (HCC) with or without liver fibrosis. (a) Immunohistochemistry for IGF2, TFF3, and AFP in human HCC and the surrounding cirrhotic tissues. Scale bar = 20 μm. (b) Expression of IGF2, TFF3, and AFP in HCC developed in non-cirrhotic and cirrhotic livers. Tumors containing clusters of cells with unequivocal cytoplasmic staining were regarded as positive (+).

EGF-dependent state to an EGF-independent, IGF2-dependent state during tumorigenesis.[31] Thus, the reactivation of *Igf2* gene expression in liver tumors might reflect the presence of continuous hepatocyte proliferation in the liver parenchyma, in which preneoplastic or neoplastic hepatocytes are eventually generated. In contrast, in the non-cirrhotic (DEN-induced and spontaneous) models, liver tumor formation may be mainly dependent on induced or spontaneous stochastic somatic mutations, which render some of the altered hepatocytes more proliferative than the surrounding intact hepatocytes. Because epigenetic alterations, including losses and gains of DNA methylation, have been increasingly recognized to occur during carcinogenesis,[32,33] we speculate that epigenetically regulated genes might serve as signatures of distinctive modes of liver tumor formation.

In conclusion, by studying transcriptome characteristics, we have shown that the mouse liver tumors induced in cirrhotic and non-cirrhotic conditions differentially reactivate various fetal/neonatal genes. In particular, our data raise the possibility that the IGF2 axis could be selectively activated in liver tumors induced by excessive proliferative stimuli following chronic liver injury.

Acknowledgments

We would like to thank Mr. Yoshiyasu Satake for animal care and Ms. Ema Yamatomi and Ms. Hiroko Chiba for secretarial assistance. We are also grateful to the staff of the Department of Pathology, Asahikawa Medical University Hospital for their generous help. This work was supported by grants from the Ministry of Education, Culture, Sports, Science, and Technology of Japan (#18590362, #21590426, and #24390092) to Yuji Nishikawa.

Disclosure Statement

The authors have no conflict of interest.

References

1 El-Serag HB. Hepatocellular carcinoma. *N Engl J Med* 2011; **365**: 1118–27.
2 Ramakrishna G, Rastogi A, Trehanpati N, Sen B, Khosla R, Sarin SK. From cirrhosis to hepatocellular carcinoma: new molecular insights on inflammation and cellular senescence. *Liver Cancer* 2013; **2**: 367–83.
3 Liu TC, Vachharajani N, Chapman WC, Brunt EM. Noncirrhotic hepatocellular carcinoma: derivation from hepatocellular adenoma? Clinicopathologic analysis. *Mod Pathol* 2014; **27**: 420–32.
4 Stoot JH, Coelen RJ, De Jong MC, Dejong CH. Malignant transformation of hepatocellular adenomas into hepatocellular carcinomas: a systematic review including more than 1600 adenoma cases. *HPB (Oxford)* 2010; **12**: 509–22.
5 Vesselinovitch SD. Infant mouse as a sensitive bioassay system for carcinogenicity of N-nitroso compounds. *IARC Sci Publ* 1980; **31**: 645–55.
6 Wang Y, Cui F, Lv Y *et al.* HBsAg and HBx knocked into the p21 locus causes hepatocellular carcinoma in mice. *Hepatology* 2004; **39**: 318–24.
7 Borlak J, Meier T, Halter R, Spanel R, Spanel-Borowski K. Epidermal growth factor-induced hepatocellular carcinoma: gene expression profiles in precursor lesions, early stage and solitary tumours. *Oncogene* 2005; **24**: 1809–19.
8 Calvisi DF, Factor VM, Ladu S, Conner EA, Thorgeirsson SS. Disruption of beta-catenin pathway or genomic instability define two distinct categories of liver cancer in transgenic mice. *Gastroenterology* 2004; **126**: 1374–86.
9 Edwards JE. Hepatomas in mice induced with carbon tetrachloride. *J Natl Cancer Inst* 1941; **2**: 197–9.
10 Gothoskar SV, Talwalkar GV, Bhide SV. Tumorigenic effect of thioacetamide in Swiss strain mice. *Br J Cancer* 1970; **24**: 498–503.
11 Andervont HB. Studies on the occurrence of spontaneous hepatomas in mice of strains C3H and CBA. *J Natl Cancer Inst* 1950; **11**: 581–92.
12 Leighton PA, Saam JR, Ingram RS, Stewart CL, Tilghman SM. An enhancer deletion affects both H19 and Igf2 expression. *Genes Dev* 1995; **9**: 2079–89.
13 Vernucci M, Cerrato F, Besnard N *et al.* The H19 endodermal enhancer is required for Igf2 activation and tumor formation in experimental liver carcinogenesis. *Oncogene* 2000; **19**: 6376–85.
14 Lederer M, Bley N, Schleifer C, Huttelmaier S. The role of the oncofetal IGF2 mRNA-binding protein 3 (IGF2BP3) in cancer. *Semin Cancer Biol* 2014; **29C**: 3–12.
15 Sell S, Becker FF, Leffert HL, Watabe L. Expression of an oncodevelopmental gene product (alpha-fetoprotein) during fetal development and adult oncogenesis. *Cancer Res* 1976; **36**: 4239–49.
16 Nordin M, Bergman D, Halje M, Engstrom W, Ward A. Epigenetic regulation of the Igf2/H19 gene cluster. *Cell Prolif* 2014; **47**: 189–99.

17 Grozdanov PN, Yovchev MI, Dabeva MD. The oncofetal protein glypican-3 is a novel marker of hepatic progenitor/oval cells. *Lab Invest* 2006; **86**: 1272–84.
18 Finkielstain GP, Forcinito P, Lui JC *et al.* An extensive genetic program occurring during postnatal growth in multiple tissues. *Endocrinology* 2009; **150**: 1791–800.
19 Okada H, Kimura MT, Tan D *et al.* Frequent trefoil factor 3 (TFF3) overexpression and promoter hypomethylation in mouse and human hepatocellular carcinomas. *Int J Oncol* 2005; **26**: 369–77.
20 Sun Q, Zhang Y, Liu F, Zhao X, Yang X. Identification of candidate biomarkers for hepatocellular carcinoma through pre-cancerous expression analysis in an HBx transgenic mouse. *Cancer Biol Ther* 2007; **6**: 1532–8.
21 Hoffmann W. Trefoil factors TFF (trefoil factor family) peptide-triggered signals promoting mucosal restitution. *Cell Mol Life Sci* 2005; **62**: 2932–8.
22 Sohda T, Yun K, Iwata K, Soejima H, Okumura M. Increased expression of insulin-like growth factor 2 in hepatocellular carcinoma is primarily regulated at the transcriptional level. *Lab Invest* 1996; **75**: 307–11.
23 Sohda T, Iwata K, Soejima H, Kamimura S, Shijo H, Yun K. In situ detection of insulin-like growth factor II (IGF2) and H19 gene expression in hepatocellular carcinoma. *J Hum Genet* 1998; **43**: 49–53.
24 Ariel I, Miao HQ, Ji XR *et al.* Imprinted H19 oncofetal RNA is a candidate tumour marker for hepatocellular carcinoma. *Mol Pathol* 1998; **51**: 21–5.
25 Boyault S, Rickman DS, de Reynies A *et al.* Transcriptome classification of HCC is related to gene alterations and to new therapeutic targets. *Hepatology* 2007; **45**: 42–52.
26 Yamamoto Y, Nishikawa Y, Tokairin T, Omori Y, Enomoto K. Increased expression of H19 non-coding mRNA follows hepatocyte proliferation in the rat and mouse. *J Hepatol* 2004; **40**: 808–14.
27 Whittaker S, Marais R, Zhu AX. The role of signaling pathways in the development and treatment of hepatocellular carcinoma. *Oncogene* 2010; **29**: 4989–5005.
28 Kato T, Miyamoto M, Date T *et al.* Repeated hepatocyte injury promotes hepatic tumorigenesis in hepatitis C virus transgenic mice. *Cancer Sci* 2003; **94**: 679–85.
29 Saenz Robles MT, Pipas JM. T antigen transgenic mouse models. *Semin Cancer Biol* 2009; **19**: 229–35.
30 Schirmacher P, Held WA, Yang D, Chisari FV, Rustum Y, Rogler CE. Reactivation of insulin-like growth factor II during hepatocarcinogenesis in transgenic mice suggests a role in malignant growth. *Cancer Res* 1992; **52**: 2549–56.
31 Stegmaier P, Voss N, Meier T, Kel A, Wingender E, Borlak J. Advanced computational biology methods identify molecular switches for malignancy in an EGF mouse model of liver cancer. *PLoS One* 2011; **6**: e17738.
32 Niwa T, Ushijima T. Induction of epigenetic alterations by chronic inflammation and its significance on carcinogenesis. *Adv Genet* 2010; **71**: 41–56.
33 Easwaran H, Tsai HC, Baylin SB. Cancer epigenetics: tumor heterogeneity, plasticity of stem-like states, and drug resistance. *Mol Cell* 2014; **54**: 716–27.

Supporting Information

Additional supporting information may be found in the online version of this article:

Fig. S1. RT-qPCR analyses of mRNA expression of Cib3, Top2a, Cdkn2b, Pnpla5, and Tspan8 in CCl_4-induced and DEN-induced liver tumors. Each value is expressed as the mean ± SEM. The numbers of samples in each group was 5, 12, 15, 6, and 13 for the CCl_4 control (olive oil), CCl_4-induced cirrhosis, CCl_4-induced tumors, DEN control, and DEN-induced tumors, respectively.

Fig. S2. The relationship between the mRNA expression of tumor-associated genes and tumor cell proliferation. Scatter plots of mRNA expression levels of the tumor-associated genes by RT-qPCR and Ki-67 labeling index (%) in CCl_4-induced tumors (n = 16) and DEN-induced tumors (n = 15). The data of the genes that were not included in Figure 4 are shown here. Spearman correlation coefficients were used to test the association between mRNA expression and tumor cell proliferation.

Table S1. Primer sequences.

Table S2. Top 10 highly-expressed genes in CCl_4-induced cirrhosis in Cluster B.